

Araştırma Makalesi - Research Article

Hegzagonal ZnO nano parçacıklarının yapısal ve elektronik özelliklerinin incelenmesi

Hasan KURBAN¹, Mustafa KURBAN^{2*}

Geliş / Received: 23/10/2019

Revize / Revised: 11/11/2019

Kabul / Accepted: 13/11/2019

ÖZ

Bu çalışmada, yoğunluk fonksiyonel sıkı bağlama (DFTB) yöntemini kullanarak, ZnO nano parçacığının yapısal ve elektronik özellikleri incelendi. İlk olarak, 258 atom içeren ~ 0.9 nm çaplı olan bir altgen kristal yapısına dayanan 30x30x30 ZnO NP karakterize edildi. İkinci olarak, ZnO nanoparçacığının HOMO, LUMO elektronik özellikleri, bant boşluğu enerjileri, Fermi seviyeleri ve durum yoğunluğu (DOS) hesaplandı. Bu özellikler ayrıca sıcaklığa bağlı olarak ta analiz edildi (en fazla 1000 K). Zn-Zn, O-O, Zn-O gibi ikili etkileşimlerin bağ sayısı, ayrılma olayları ve radyal dağılım fonksiyonu (RDF) gibi yapısal analiz, yeni algoritmalar kullanılarak incelendi. Sonuçlarımız, Zn-Zn bağlarının sayısının O-O ve Zn-O bağlarından daha fazla olduğunu göstermektedir; bu nedenle, Zn atomlarının Zn atomları ile bağ yapmayı daha çok tercih ettiği görülmektedir. Ayrıca durum yoğunluğunu (DOS) analiz ettik ve ZnO parçacığının yarı iletken benzeri bir karakter gösterdiğini gözlemledik. Sıcaklığa bağlı, HOMO-LUMO enerji boşluğu arttığı görüldü. Ayrıca, sonuçların deneysel verilerle uyumlu olduğu bulundu.

Anahtar Kelimeler- *Zno, Nano Parçacıklar, Bant Aralığı, Elektronik Yapı, DFTB.*

^{2*}Sorumlu yazar iletişim: mkurbanphys@gmail.com (<https://orcid.org/0000-0002-7263-0234>)

Department of Electronics and Automation, Kırşehir Ahi Evran University, 40100 Kırşehir, TURKEY.

¹İletişim: hakurban@gmail.com (<https://orcid.org/0000-0003-3142-2866>)

School of Information, Computing and Engineering, Indiana University, Bloomington, 47405 Indiana, USA.

Study of Structural and Optoelectronic Properties of Hexagonal ZnO Nanoparticles

ABSTRACT

In this work, we used the density-functional tight-binding (DFTB) and investigate ZnO nanoparticle (NP) properties, i.e., the structural and electronic properties. First, a ZnO NP with ~ 0.9 nm including 258 atoms was characterized from $30 \times 30 \times 30$ supercell based on the hexagonal crystal structure of ZnO. Second, HOMO, LUMO electronic properties, bandgap energies, Fermi levels and density of states (DOS), of the ZnO NP were calculated. These properties were also analyzed in terms of temperature (up to 1000 K). The structural analysis, such as the number of bonds, segregation phenomena and radial distribution function (RDF) of two-body interactions such as Zn-Zn, O-O, Zn-O were investigated using novel algorithms. Our results demonstrate that the number of Zn-Zn bonds is greater than that of O-O, and Zn-O bonds; thus, it appears that Zn atoms have a greater preference for Zn atoms. We also analyzed the density of state (DOS) and observed that ZnO NP demonstrate a semiconductor-like character. The HOMO-LUMO energy gap increases while the temperature goes up. The results are found to be compatible with experimental data.

Keywords- *Zno, Nanoparticles, Bandgap, Electronic Structure, DFTB.*

I. INTRODUCTION

Recently, nanoparticles (NPs), tiny objects whose sizes are lay between 1 and 100 nanometers, have found use in many areas such as energy, electronics, biomedical and optical fields due to their shape dependence properties as opposed to their bulk structure. More specifically, metallic NPs exhibit properties useful as both insulators and semiconductors and have been widely investigated [1-3]. ZnO NPs, in particular, have been an area of intense scrutiny, because they have a wide bandgap and excellent optical properties for optoelectronics applications, being widely studied in various fields as photodetectors [4], energetic materials [5], and biomedical agents [6]. Moreover, an atom substitution on the materials has recently become a hot topic [7]. Herein, many studies have been performed on the X-doped ZnO ($X = \text{Mn}$ and Zn) and pure ZnO NPs [8-10] or even ZnO doped-amorphous carbon [11].

In this work, we use the DFTB method to observe the effect of temperature on a ZnO NP model. Among the analyses we conduct are studies of electronic features such as the HOMO, LUMO, HOMO-LUMO gap (E_g) and total energies, density of states (DOS), as well as, structural analysis such as radial distribution function (RDF), order parameter (R) to learn about how behave Zinc (Zn) and Oxygen (O) atoms based on temperature and the number of bonds (n) of two-body interactions in the ZnO NP. To supplement our work on structural analysis, we implemented programs in R code (<https://github.com/hasankurban/Structural-Analysis-NanoParticles>) to analyze the RDF, n and R .

II. MATERIAL AND METHOD

We used the DFTB+ code [12], which is an implementation of DFTB method, with the 3ob/3ob-3-1 [13, 14] set of Slater Koster parameters to understand the structural features and electronic structure of ZnO NP. To make the program more accessible to users, we have also ensured that the programs are simple to use. Additionally, we have added functionality to include analysis of the RDF, n and R of the ZnO NP based on an increase in temperature. The code open source is freely available online, thus, researchers can visualize their data using the code.

III. RESULTS AND DISCUSSION

A. Structural Analysis

The initial structure of ZnO NP with $n = 258$ atoms is shown in Figure 1. The ZnO NP was characterized by $30 \times 30 \times 30$ supercells of the hexagonal crystal structure (wurtzite, space group $P6_3mc$). We carved a spherical ZnO NP from this bulk hexagonal supercell. The radius of the NP is set to a desired value (0.9 nm) and only atoms within that sphere are considered, whereas those outside the sphere are removed. We performed all calculations at constant volume.

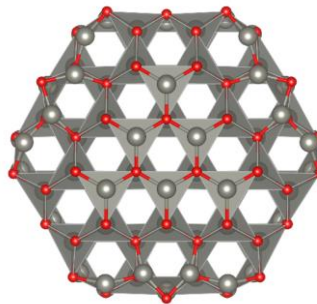


Figure 1. Initial structure (polyhedral) of ZnO NP with 258 atoms. (Red is Oxygen, grey is Zinc).

The n_{ij} represents the nearest neighbor contacts number, which is also the number of bonds, and usually used to distinguish the degree of packing, a significant property of NP. The n_{ij} [15] number for the NP can be calculated as follows:

$$n_{ij} = \sum_{i < j} \delta_{ij} \quad (1)$$

where $\delta_{ij} = \begin{cases} 1, r_{ij} \leq 1.2r_{ij}^{(0)} \\ 0, r_{ij} > 1.2r_{ij}^{(0)} \end{cases}$ $i, j = \text{Zn, or O}$, r_{ij} is the distance between atom i and j and $r_{ij}^{(0)}$ is obtained

by fitting the experimental data and represents a nearest neighbor criterion [16, 17]. Figure 2 indicates the total n in the ZnO NP with 258 atoms. The curve of ZnO NP in Fig. 2 reveals that the number of O-O bonds decreases gradually in terms of an increase in temperature in the ZnO NP. Moreover, the total n of Zn-Zn interactions is comparatively smaller than total n , while the n of O-O is the smallest. This result shows that Zn atoms incline to form more bonds with Zn atoms: that Zn₂ tends to the surface. Additionally, the total n of Zn-Zn is larger than that of Zn-O and O-O; thus, one can conclude that O atoms have higher priority for Zn atoms than O atoms based on the increase in temperature.

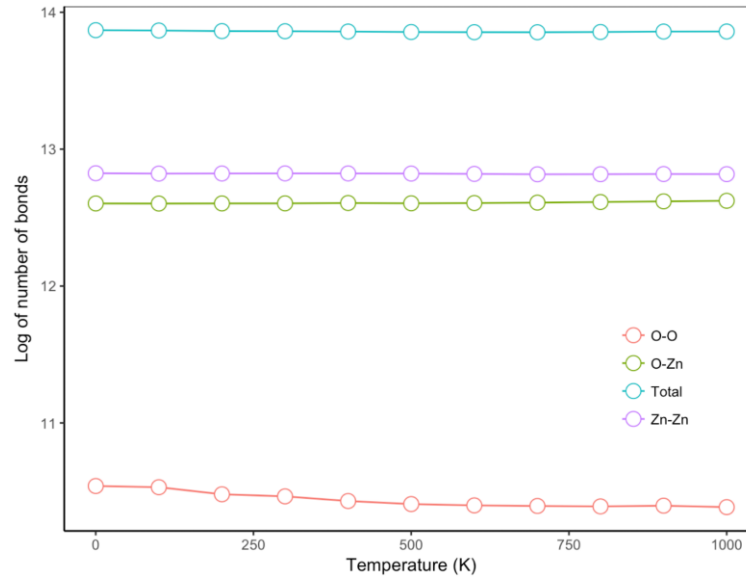


Figure 2. The changes in the n of Zn-O, O-O and Zn-Zn interactions based on an increase in the ZnO NP.

The R_T represents the order parameter and is used to find a stable structure in the NP. One needs to calculate R_T [18-22] which helps to investigate the segregation of atoms in the NP. R_T is the average distance of a type T_i atoms according to a center of a NP,

$$R_{T_i} = \frac{1}{n_{T_i}} \sum_{i=1}^{n_{T_i}} r_i \quad (2)$$

where n_T is the number of T_i type atoms, and r_i is the distance of the atoms to the coordinate center. We define a distance from the center of NP to a reference point as ϵ to indicate the location of atoms; if $R_T < \epsilon_{min}$ (a “small” value), the T_i type atoms are assumed to be at the center, and if $R_T > \epsilon_{max}$ (a “large” value), the T_i type atoms are assumed to be at the surface region of NP. If neither is true, *i.e.*, if $\epsilon_{min} < R_T < \epsilon_{max}$ (a “medium” value), it is assumed a well-mixed NP.

Fig. 3 demonstrates the behavior of R of Zn and O atoms with respect to temperature. Here, the R shows the changes in the structural properties of ZnO NP with a change in temperature. For example, the R of Zn and O atoms indicates that O and Zn atoms slightly tend to locate at the center until 500 K, while Zn atoms sharply

tend to occupy at the center after about 750 K. On the other hand, the R of O atoms to the surface is related to its lower cohesive energy when compared to Zn.

The Radial Distribution Function (RDF), a significant parameter, is known as the probability of finding a particle at a distance r from another tagged particle. The RDF is calculated as follows: $g(r_i) = n(r_i) / (|\Delta| \times V_s \times V_d)$ where $n(r_i)$ represents the mean number of atoms in a shell of width dr at distance r_i , $|\Delta|$ is the total number of atoms and V_s and V_d are the volume of the spherical shell and the mean atom density, respectively.

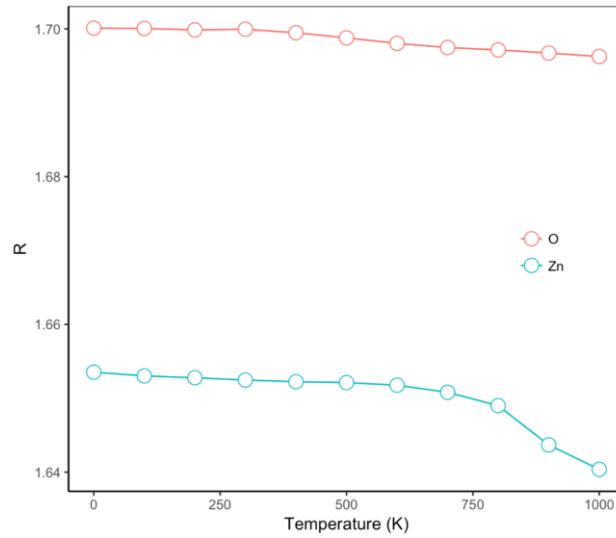


Figure 3. While changing temperature, how the order parameters of Zn and O atoms in the ZnO NP vary.

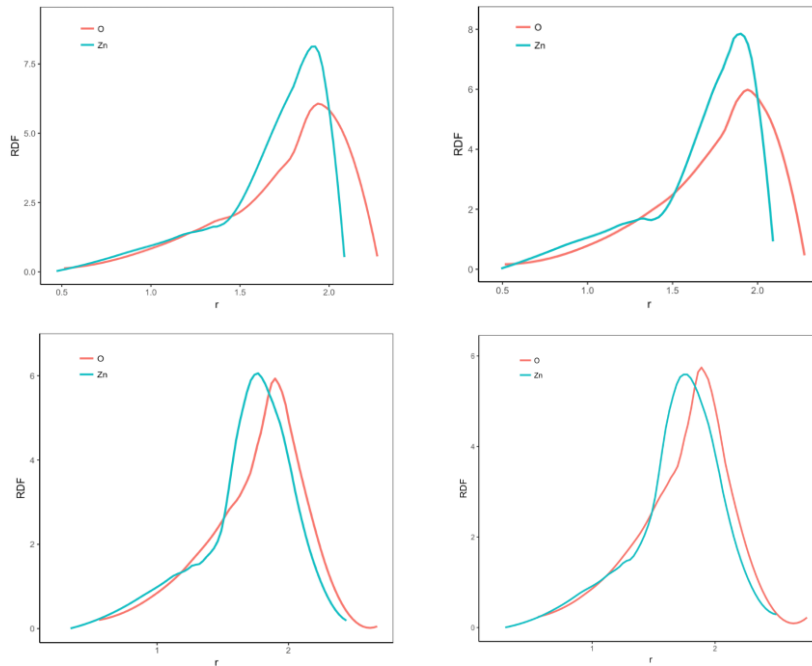


Figure 4. Radial distribution function of the ZnO NP at 0, 100, 900 and 1000K.

Fig. 4 shows the RDF Zn-Zn and O-O binary interactions in the ZnO NP. The RDFs are performed for each binary interaction in the optimized structures. Our results show that Zn-Zn has a narrower and higher distribution than O-O interactions at low temperatures. With regards to an increase in temperature, distribution of the peaks for both pairs. Moreover, the distribution of O atoms increased by raising the temperature due to a decrease in the total n of O-O interactions.

B. Electronic structure

In Fig. 5, we demonstrate the results of the HOMO, LUMO and Fermi levels with respect to temperature to acquire detailed information on electronic states in the ZnO NP. Our results indicate that the ZnO NP has the energy gap, so it shows semiconductor character. While increasing the temperature, we observe that LUMO and Fermi energy increases whereas the HOMO level decreases. The HOMO value for the ZnO NP is -7.89 eV wide at 0 K, *i.e.*, approximately 0.28 eV larger than that of about 1000K, which has the lowest HOMO value (-6.91 eV) and is less reactive, while being more stable than that of lower temperature (see Fig. 5). Fermi energy levels are in the middle of the valence and conduction band. The HOMO-LUMO energy gap of ZnO NP is 4.71 eV at 0 K, which decreases from 4.71 to 2.42 eV (see Fig. 6) with an increase in temperature which gives rise to a lattice expand, thus it induces to an increase in electron-phonon interaction. Herein, one can conclude that the expansion in lattice constant causes a decrease in the energy gap. It is clear then that an increase in temperature helps ZnO NP destabilize due to a decrease in the energy gap, thus ZnO NP at a lower temperature can be preferred for the application of electronic devices because the electronic transfer is easier.

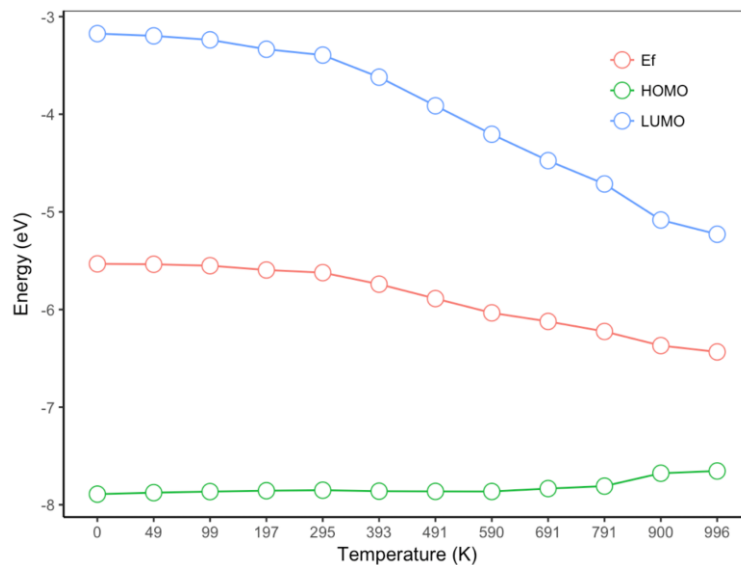


Figure 5. While changing temperature, how HOMO, LUMO and Fermi energies of ZnO NP alternates.

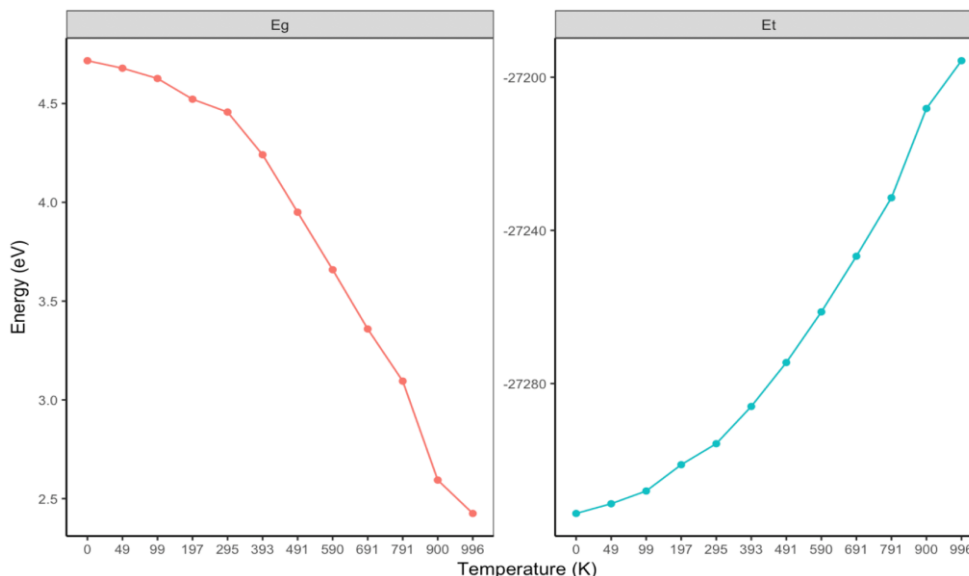


Figure 6. HOMO-LUMO energy gap and total energy ZnO NP in terms of temperature.

IV. SONUÇLAR

In this work, we use the DFTB method and study electronic structure and structural properties of a ZnO NP with 258 atoms. We also developed new code in R to conduct structural analysis, i.e., analyzing the RDF, n and R of two-body interactions of atoms in the ZnO NP. We also observe that while increasing temperature, the ZnO NP stabilize better. The segregation of Zn and O atoms indicates that Zn atoms tend to locate at the center, while O atoms tend to occupy the surface as a general trend. The total n of Zn-Zn interactions is larger than that of O-O and Zn-O; thus, one can conclude that Zn atoms have a greater preference for Zn atoms rather than O atoms. The R of Zn and O atoms indicates a tendency to locate at the center. The HOMO energy level decreases; however, the LUMO level increase, thus the HOMO-LUMO band gap decreases from 4.717 to 2.425 eV due to an increase in electron-phonon interaction. The decrease in the HOMO levels helps ZnO NP to stabilize. The ZnO NP at high temperature is desirable in energy.

ACKNOWLEDGMENTS

The numerical calculations were also partially performed at TUBITAK ULAKBIM, High Performance and Grid Computing Centre (TRUBA resources), Turkey.

REFERENCES

- [1] Wang, C. L., Zhang, H., Zhang, J. H., Li, M. J., Sun, H. Z., & Yang, B. (2007). Application of Ultrasonic Irradiation in Aqueous Synthesis of Highly Fluorescent CdTe/CdS Core-Shell Nanocrystals. *J. Phys. Chem. C* 111, 2465-2469.
- [2] Yang, P., Tretiak, S., Masunov, A. E., & Ivanov, S. (2008). Quantum chemistry of the minimal CdSe clusters. *J. Chem. Phys.* 129, 074709 (1–12).
- [3] Kushwaha, A. K. (2012). Lattice dynamical calculations for HgTe, CdTe and their ternary alloy Cd_xHg_{1-x}Te. *Comp. Mater Sci.* 65, 315-319.
- [4] Chang S-P., & Chen, K-J. (2012). Zinc Oxide NP Photodetector. *J. Nanomater.* 2012, 1-5.

- [5] Barzinjy, A. A., Mustafa, S., & Ismael, H. H. J. (2019). Characterization of ZnO NPs Prepared from Green Synthesis Using Euphorbia Petiolata Leaves. *EAJSE* 4, 74-83.
- [6] Zhang, Y., Nayak, T. R., Hong, H., & Cai, W. (2013). Biomedical applications of zinc oxide nanomaterials. *Curr. Mol. Med.* 13(10), 1633-1645.
- [7] Kurban, M. (2018). Electronic structure, optical and structural properties of Si, Ni, B and N-doped a carbon nanotube: DFT study. *Optik* 172, 295-301.
- [8] Rezkallah, T., Djabri, I., Koç, M. M., Erkovan, M., Chumakov, Y., & Chemam F. (2017). Investigation of the electronic and magnetic properties of Mn doped ZnO using the FP-LAPW method. *Chin. J. Phys.* 55, 1432-1440.
- [9] Akgül, G., & Akgül, F. A. (2019). Kobalt Katkılı Çinko Oksit Nanoparçacıklarının Yapısal Özelliklerinin İncelenmesi. *Selcuk Univ. J. Eng. Sci. Tech.* 7, 105-114.
- [10] Akgül, G., Akgül, F. A., Attenkofer, K., & Winterer, M. (2013). Structural properties of zinc oxide and titanium dioxide nanoparticles prepared by chemical vapor synthesis. *J. Alloys Compd.* 554, 177-181.
- [11] Koç, M. M., Aslan, N., Erkovan, M., Aksakal, B., Uzun, O., Farooq, W. A., & Yakuphanoglu, F. (2019). Electrical Characterization of Solar Sensitive Zinc Oxide Doped-Amorphous Carbon Photodiode. *Optik* 178, 316-326.
- [12] Aradi, B., Hourahine, B., & Frauenheim, T. (2007). DFTB+, a Sparse Matrix-Based Implementation of the DFTB Method. *J. Phys. Chem. A* 111, 5678-5684.
- [13] Gaus, M., Goez, A., & Elstner, M., (2013). Parametrization and Benchmark of DFTB3 for Organic Molecules. *J. Chem. Theory Comput.* 9, 338-354.
- [14] Kubillus, M., Kubař, T., Gaus, M., Řezáč, J., & Elstner, M. (2015). Parameterization of the DFTB3 Method for Br, Ca, Cl, F, I, K, and Na in Organic and Biological Systems. *J. Chem. Theory Comput.* 11, 332-342.
- [15] Wu, X., Wei, Z., Liu, Q., Pang, T., & Wu, G. (2016). Structure and bonding in quaternary Ag-Au-Pd-Pt clusters. *J Alloy. Compd.* 687, 115-120.
- [16] NIST Standard Reference Database (2019). Experimental bond lengths. <https://cccbdb.nist.gov/expbondlengths1.asp>.
- [17] Czajkowski, M. A., & Koperski, J. (1999). The Cd₂ and Zn₂ van der Waals dimers revisited. Correction for some molecular potential parameters. *Spectrochim. Acta, Part A* 55, 2221-2229.
- [18] Kurban, M., Malcıođlu, O. B., & Erkoç, Ş., (2016). Structural and thermal properties of Cd-Zn-Te ternary NPs: Molecular-dynamics simulations. *Chem. Phys.* 464, 40-45.
- [19] Kurban, M. (2018). Size and composition dependent structure of ternary Cd-Te-Se nanoparticles. *Turk. J. Phys.* 42, 443-454.
- [20] Kurban, H., Kurban, M., & Dalkılıç, M. (2019). Density-functional tight-binding approach for the structural analysis and electronic structure of copper hydride metallic nanoparticles, *Mater. Today Commun.* 21, 100648(1-7).
- [21] Kurban, M. (2018). Molecular Dynamics study on the structural, thermal and energetic properties of GaAs Nanoparticles, *ESTUJST-A*, 19(3), 620-627.
- [22] Kurban, M., & Erkoç, Ş. (2017). Segregation formation, thermal and electronic properties of ternary cubic CdZnTe clusters: DFT calculations and MD simulations, *Physica E*, 88, 243-251.